Electronic Supplementary Material (ESI) for ChemComm.

Supporting Information for:

Catalytic Hydrogenation Enabled by Ligand-Based Storage of Hydrogen

Andrew J. McNeece[†], Kate A. Jesse[†], Alexander S. Filatov, Joseph E. Schneider, and John S. Anderson*

*jsanderson@uchicago.edu

[†]These authors contributed equally

Table of Contents

NMR Spectra

UV-vis Spectra

IR Spectra

Kinetics Studies

DFT Calculations

X-Ray Crystallography

Mass Spectrometry

Experimental

General Considerations: All reagents were purchased from commercial suppliers and used without further purification unless otherwise specified. Compound **3** was synthesized as previously reported.[1] All manipulations were carried out under an atmosphere of N_2 using standard Schlenk and glovebox techniques. Glassware was dried at 180 °C for a minimum of two hours and cooled under vacuum prior to use. Solvents were dried on a solvent purification system from Pure Process Technology and stored over 4 Å molecular sieves under N_2. Tetrahydrofuran was stirred over NaK alloy and run through an additional activated alumina column prior to use to ensure dryness. Solvents were tested for H_2O and O_2 using a standard solution of sodium-benzophenone ketyl radical anion. C_6D_6 was dried by passage over a column of activated alumina and stored over 4 Å molecular sieves in the glovebox. ^1H, $^{13}C\{^1H\}$, and $^{19}F\{^1H\}$ spectra were recorded on Bruker DRX 400 or 500 spectrometers. Chemical shifts are reported in ppm units referenced to residual solvent resonances for ^1H and $^{13}C\{^1H\}$ spectra, UV-vis spectra were recorded on a Thermo Evolution 300 spectrometer and addition of gases was performed by injecting via syringe into a cuvette sealed with a septum. UV-visible spectra at elevated temperature were done using a Unisoku Cryostat. IR was recorded on a Bruker Tensor II. GC/MS was collected on an Agilent SQ GCMS with 5977A single quad MS and 7890B GC. Elemental analysis was performed by Midwest Microlabs. Electrochemical measurements were performed using a BAS Epsilon potentiostat and analyzed using BAS Epsilon software version 1.40.67NT. Cyclic voltammetry measurements were made using a glassy carbon working electrode, platinum wire counter electrode, and silver wire pseudo-reference electrode, and referenced to internal Fc/Fc^+.

X-Ray Structure Determination. Crystal Structure Determination. The diffraction data were measured at 100 K on a Bruker D8 VENTURE with PHOTON 100 CMOS detector system equipped with a Mo-target micro-focus X-ray tube (λ = 0.71073 Å) or at the Advanced Photon Source of Argonne National Laboratory (beamline 15-ID-B,C,D) using X-ray radiation with a wavelength of λ = 0.41328 Å. Data reduction and integration were performed with the Bruker APEX3 software package (Bruker AXS, version 2015.5-2, 2015). Data were scaled and corrected for absorption effects using the multi-scan procedure as implemented in SADABS (Bruker AXS, version 2014/5, 2015, part of Bruker APEX3 software package). The structure was solved by the dual method implemented in SHELXT[2] and refined by a full-matrix least-squares procedure using OLEX23[3] software package (XL refinement program version 2014/7[4]). Suitable crystals were mounted on a cryo-loop and transferred into the cold nitrogen stream of the Bruker D8 Venture diffractometer. Most of the hydrogen atoms, with the exception of N–H protons which were located in the difference map, were generated by geometrical considerations and constrained to idealized geometries and allowed to ride on their carrier atoms with an isotropic displacement parameter related to the equivalent displacement parameter of their carrier atoms.

Synthesis of ($^{t\mathrm{Bu,Tol}}$DHPH$_2$)NiCl (1). To a stirring THF solution of $^{t\mathrm{Bu,Tol}}$DHP•2HCl (0.105 g, 0.200 mmol, 15 mL) was added *n*-BuLi (2.0 M in hexanes, 0.23 mL, 0.59 mmol, 2.9 eq) which resulted in a color change to clear red. This solution was then added dropwise to a stirring THF solution of (dme)NiCl$_2$ (0.045 g, 0.20 mmol, 1 eq, 3 mL) resulting in a reddish/tan solution. This was stirred for 2 hours, then filtered and all volatiles were removed in-vacuo. The resulting red oil was washed with petroleum ether (10 mL), resulting in (^{tBu,Tol}DHPH$_2$)NiCl as a tan powder. Single crystals could be obtained by crystallization of the petroleum ether wash at –35 °C Yield: 0.060 g, 56%. ^{1}H NMR (C_6D_6, 400 MHz, 25° C) δ = 7.87 (d, *J* = 8 Hz, 4H, Tol C–H), 7.06 (d, *J* = 8 Hz, 4H, Tol C–H), 6.55 (s, 2H, Pyrrole C–H), 5.99 (s, 2H, N–H), 2.12 (s, 6H, Tol-CH_3), 1.19 (s, 18H, *t*Bu-CH_3). ^{13}C{^{1}H} NMR (C_6D_6, 125 MHz, 25° C) δ = 166.84, 141.15, 134.94, 130.56, 129.97, 129.49, 119.93, 64.78, 29.09, 21.67. UV-vis, nm in THF (ε, M^{-1}cm^{-1}): 362 (8806). IR (cm^{-1}, THF solution, CaF_2 windows): 3241 (w, N–H), 3166 (m, N–H), 618 (w), 1585 (m, C=N), 1553 (m), 1470 (s), 1364 (s), 1314 (m), 1250 (m), 1179 (s), 1131 (w). HRMS (ESI) Calc'd for $[M+H]^+$: 536.2091 Found: 536.2058. Anal Calc'd (**1** + pentane) C 65.1 H 7.95 N 11.5 Found C 65.5, H 6.7 N 12.4.*

Synthesis of (^{tBu,Tol}DHPH$_2$)NiOTf (2) To a stirring THF solution of (^{tBu,Tol}DHPH$_2$)NiCl (0.025 g, 0.040 mmol, 5 mL) was added a THF solution of AgOTf (0.012 g, 0.047 mmol, 1.2 eq, 2 mL), resulting in immediate precipitation of a white powder. The reaction was stirred for 20 minutes, then filtered and all volatiles were removed *in vacuo*, giving [(^{tBu,Tol}DHPH$_2$)Ni]OTf as an oily yellow residue. Yield: 0.026 g, 90%. Single crystals could be obtained by slow evaporation of diethyl ether at room temperature overnight. ^{1}H NMR (C_6D_6, 400 MHz, 25° C) δ = 7.78 (d, *J* = 8 Hz, 4H, Tol C–H), 7.05 (d, *J* = 8 Hz, 4H, Tol C–H), 6.45 (s, 2H, Pyrrole C–H), 6.25 (s, 2H, N–H), 2.11 (s, 6H, Tol-CH_3), 1.15 (s, 18H, *t*Bu-CH_3). ^{13}C{^{1}H} NMR (C_6D_6, 125 MHz, 25° C) 166.2, 140.9, 133.5, 129.8, 128.8, 120.3, 64.9, 27.3, 20.9. ^{19}F{^{1}H} NMR (C_6D_6, 125 MHz, 25° C) –77. UV-vis, nm in THF (ε, M^{-1}cm^{-1}): 356 (8508). IR (cm^{-1}, THF solution, CaF_2 windows): 3250 (w, N–H), 3197 (m, N–H), 1615 (w), 1588 (s, C=N), 1483 (w), 1381 (m), 1337 (s), 1209 (w). HRMS (ESI) Calc'd for $[M+H]^+$: 650.1923 Found: 650.1891. Anal Calc'd (**2** + THF) C 54.9 H 6.1 N 9.7 Found C 54.2 H 6.6 N 9.5.*

*Complexes **1** and **2** are both extremely greasy or co-crystallize with solvent making them difficult to rigorously dry. Combustion analysis routinely gives values different than theory and potentially more consistent with solvates. Nevertheless, the combination of data acquired supports the assignment and purity of these species.

Synthesis of 2 via H_2 splitting from 3. A C_6D_6 solution of **3** was removed from the glovebox in a J-young NMR tube, degassed via three freeze-pump-thaw cycles, and placed under an atmosphere of H_2. After two hours at room temperature **2** appeared in the ^{1}H NMR, and after heating the reaction to 50 °C overnight full conversion to **2** was observed.

Synthesis of 3 via hydrogenation of Benzoquinone. A solution of **2** (0.0007 g, 0.001 mmol) in d_8-toluene was combined with benzoquinone (0.0015 g, 0.013 mmol, 13 eq) in a J-young NMR tube. This was monitored by ^{1}H NMR over the next week for conversion to **3**.

Catalytic Reaction of 3 with Benzoquinone.

By ^{1}H NMR: A C_6D_6 solution of **3** (0.005 g, 0.0077 mmol) and benzoquinone (0.0025 g, 0.02 mmol, 3 eq) was removed from the glovebox in a J-young NMR tube, degassed via three freeze-pump-thaw cycles, and placed under an atmosphere of H_2. Monitoring by ^{1}H NMR showed the slow appearance of **2** and ~2 eq of hydroquinone over the course of two days at room temperature based on integration.

By GC-MS: A d_8-toluene solution of **3** (0.003 g, 0.0046 mmol) and benzoquinone (0.010 g, 0.09 mmol, 20 eq) was removed from the glovebox in a J-young NMR tube, degassed via three freeze-pump-thaw cycles, and placed under an atmosphere of H_2. Monitoring by ^{1}H NMR showed the slow appearance of **2** and hydroquinone over the course of 7 days at room temperature. The solution was dried, dissolved in DCM, and filtered for GCMS. The relative integrations of peaks in the chromatogram corresponding to benzoquinone and hydroquinone to determine that of the 20 eq. of benzoquione added to the reaction mixture, ~2 equivalents had been hydrogenated to hydroquinone.

GC-MS Controls:

1. A d_8-toluene solution benzoquinone (0.010 g, 0.09 mmol) was removed from the glovebox in a J-young NMR tube, degassed via three freeze-pump-thaw cycles, and placed under an atmosphere of H_2. Monitoring by ^{1}H NMR showed no appearance of hydroquinone over the course of 7 days at room temperature. The solution was dried, dissolved in DCM, and filtered for GCMS. A peak corresponding to benzoquinone was observed, but no peak corresponding to hydroquinone was observed.
2. GC-MS was collected on a solution of benzoquinone in DCM.
3. GC-MS was collected on a solution of hydroquinone in DCM.

Kinetics of H_2 splitting. In a 20 mL vial in the glovebox, a 2 mM stock solution of **3** was prepared by dissolving 5.6 mg of crystalline complex in 4 mL of THF. This was used to prepare either 0.4 mM or 0.2 mM samples used for UV-vis by dilution and was stored at −35 °C between experiments. Each sample was transferred to a standard 1 cm cuvette under nitrogen. This was then placed in a Unisoku CoolSpek cryostat set at 30, 40, 50, or 60 °C. The solution was allowed to equilibrate for 5 minutes prior to collection of an initial spectrum of the sample. Immediately after this 0.5 mL of H_2 (0.02 mmol, 25 equiv. (0.4 mM samples) or 50 equiv. (0.2 mM samples)) was syringed into the cuvette and bubbled through the UV-vis solution. Spectra were collected for a minimum of 2 half-lives. Experiments were done in triplicate for each temperature.

Data Analysis: Eyring Analysis

The intensity of the absorbance at 650 nm was plotted against time in seconds then fit using an exponential function in Origin 8.5 to obtain the rate for each experiment. The rates at each temperature were averaged and the standard deviation was determined. This was used for an Eyring analysis where the standard deviation of the rate at each temperature is shown as vertical error bars.

NMR Spectra

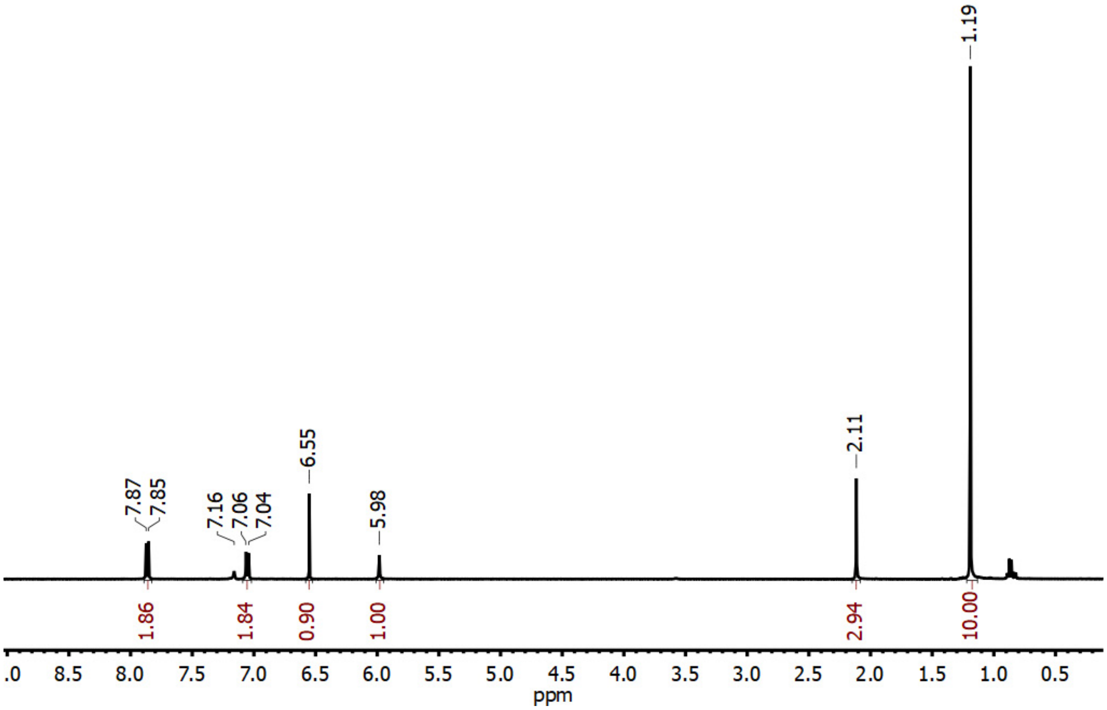

Figure S1. ^{1}H NMR of **1** in C_6D_6.

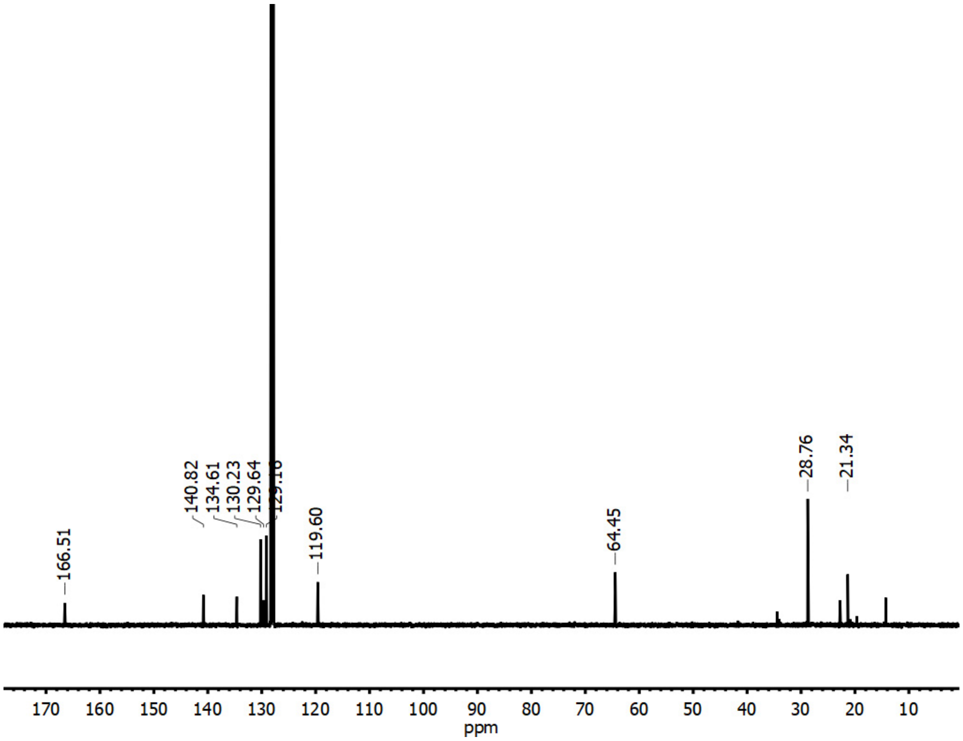

Figure S2. $^{13}C\{^{1}H\}$ NMR of **1** in C_6D_6.

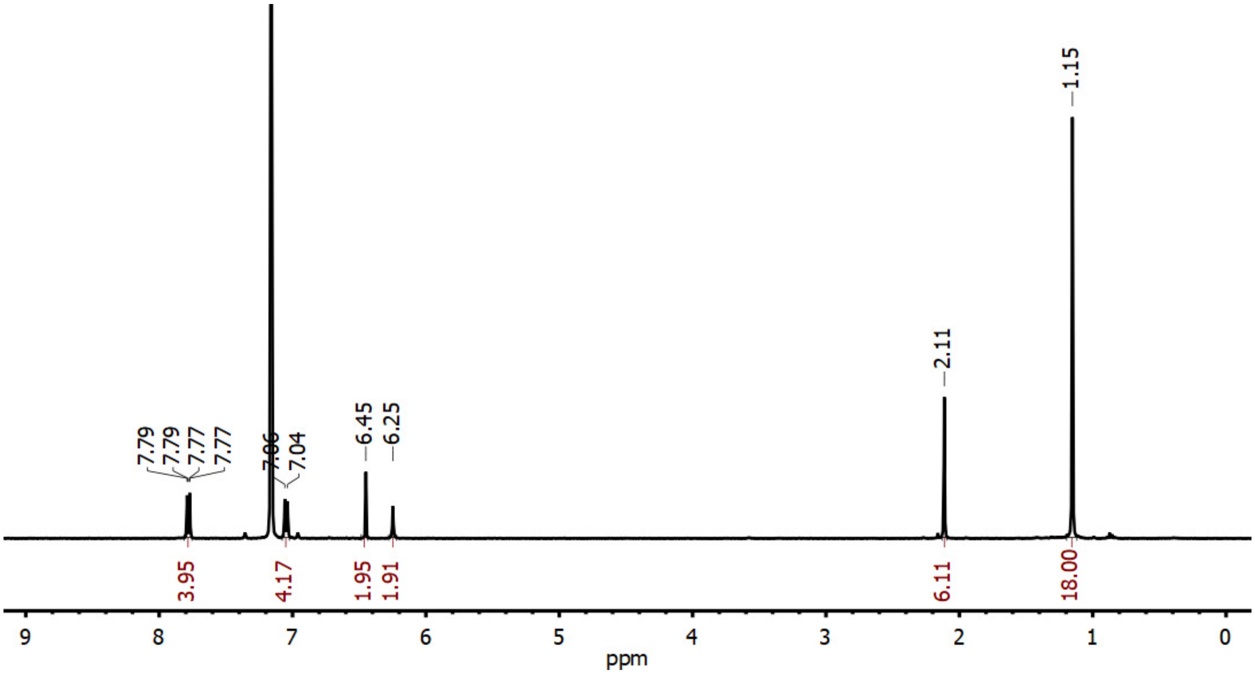

Figure S3. ^{1}H NMR of **2** in C_6D_6.

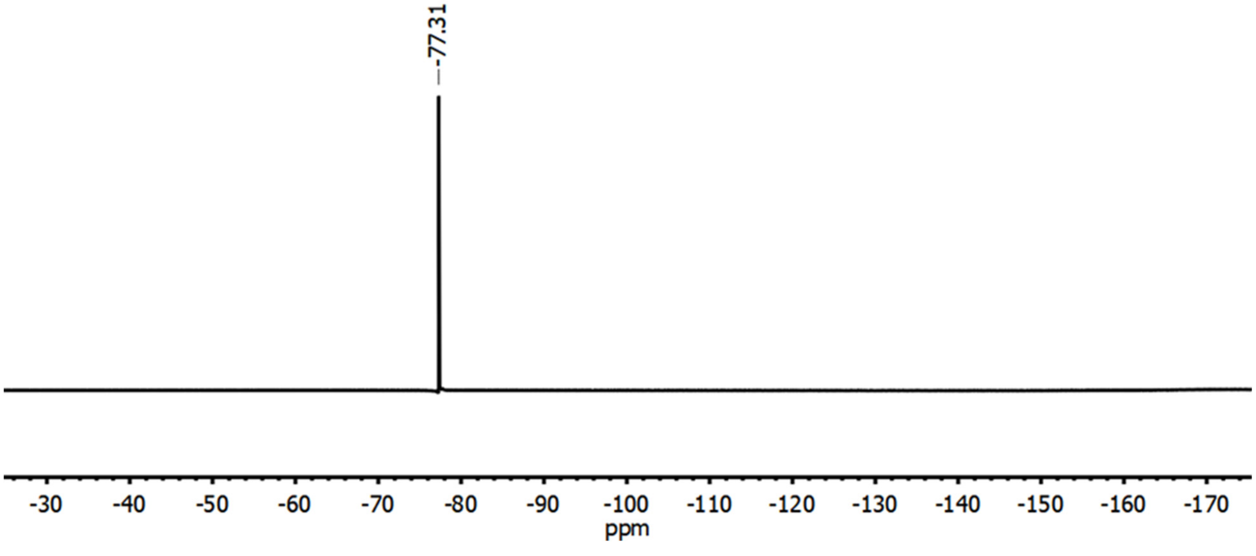

Figure S4. $^{19}F\{^1H\}$ NMR of **2** in C_6D_6.

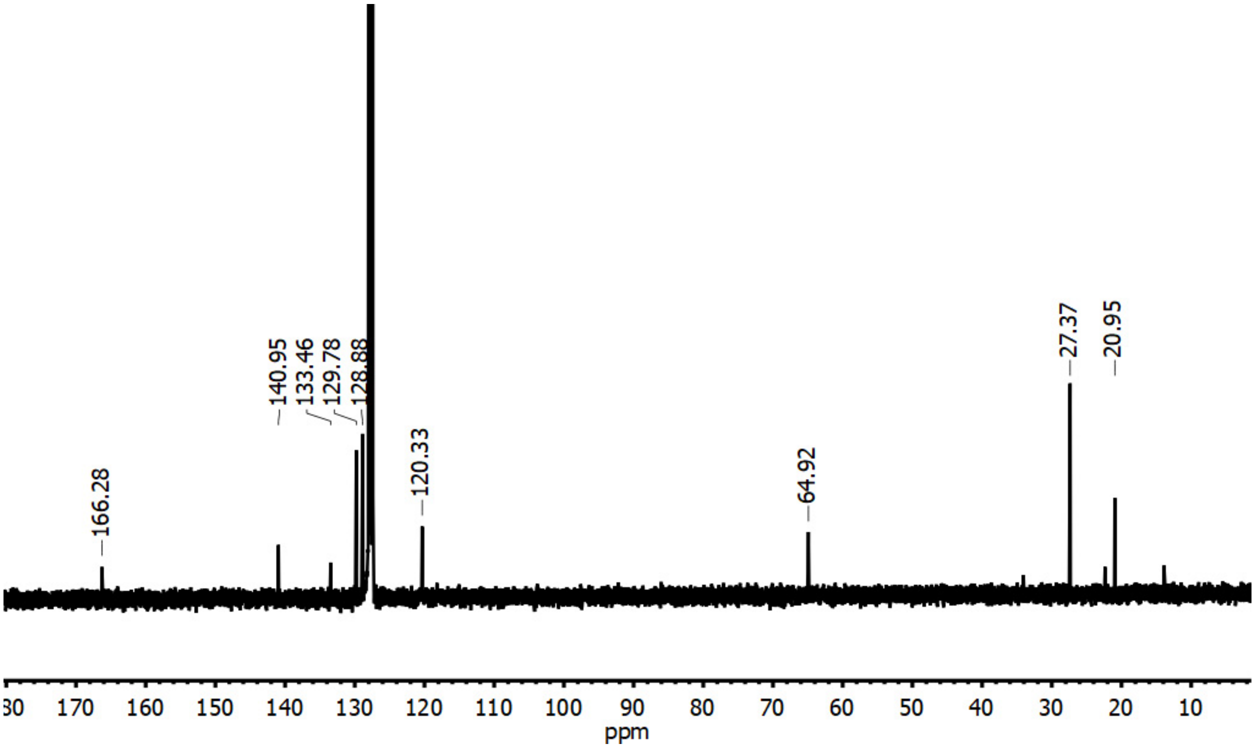

Figure S5. $^{13}C\{^1H\}$ NMR of **2** in C_6D_6.

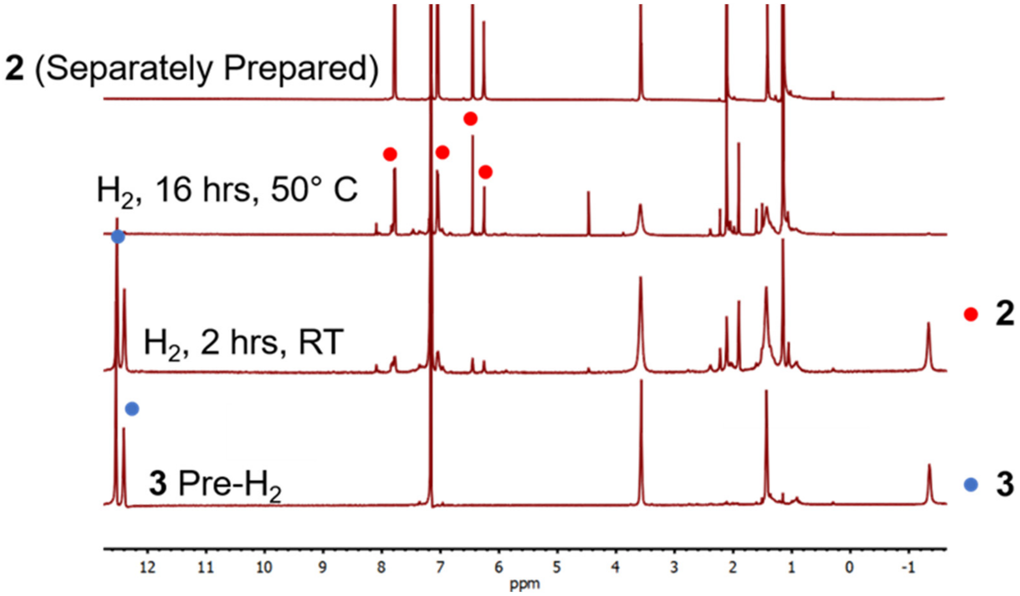

Figure S6. ^1H NMR in C_6D_6 of H_2 splitting by **3** to form **2**.

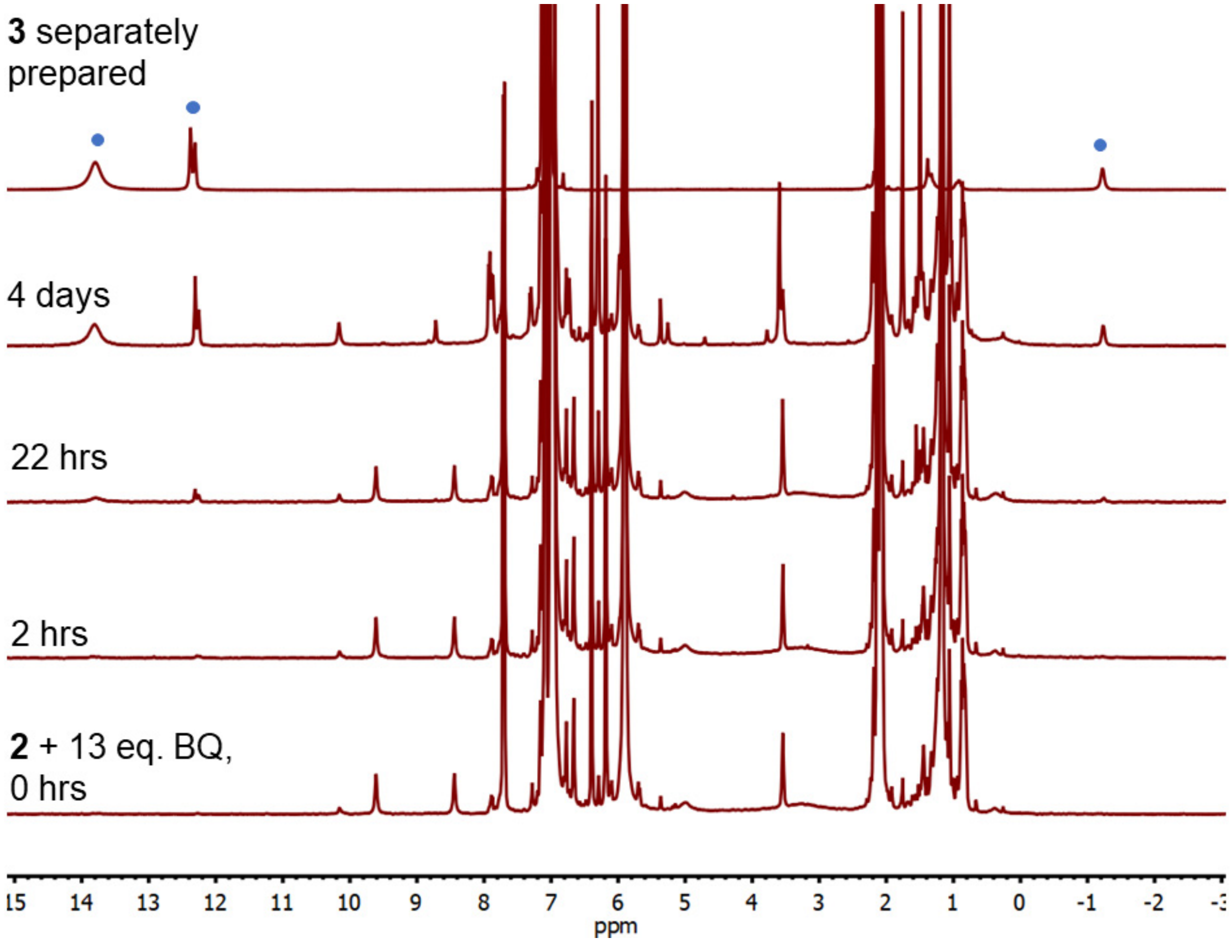

Figure S7. ^{1}H NMR in d_8-toluene of the transformation of **2** to form **3** in the presence of 13 eq benzoquinone (BQ).

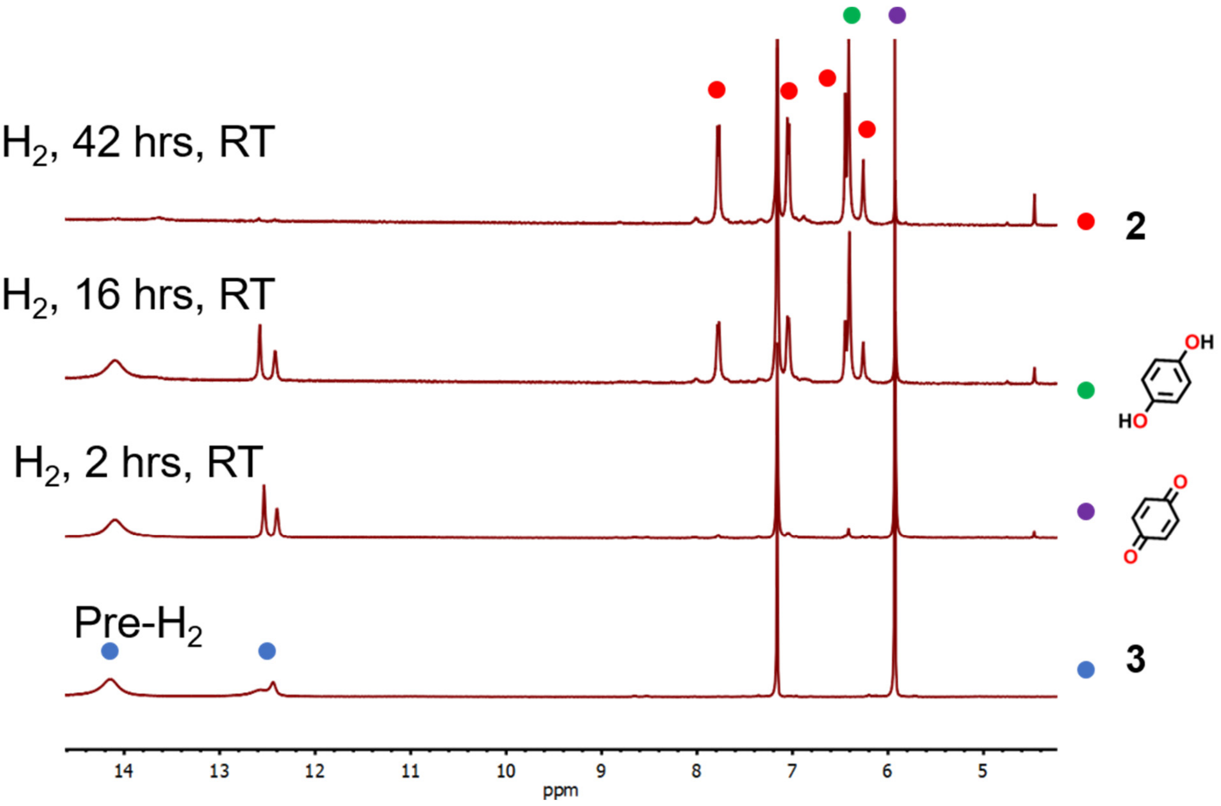

Figure S8. ^{1}H NMR of the reaction of **2** with H$_2$ and benzoquinone showing appearance of **2** and 2 equivalents of hydroquinone.

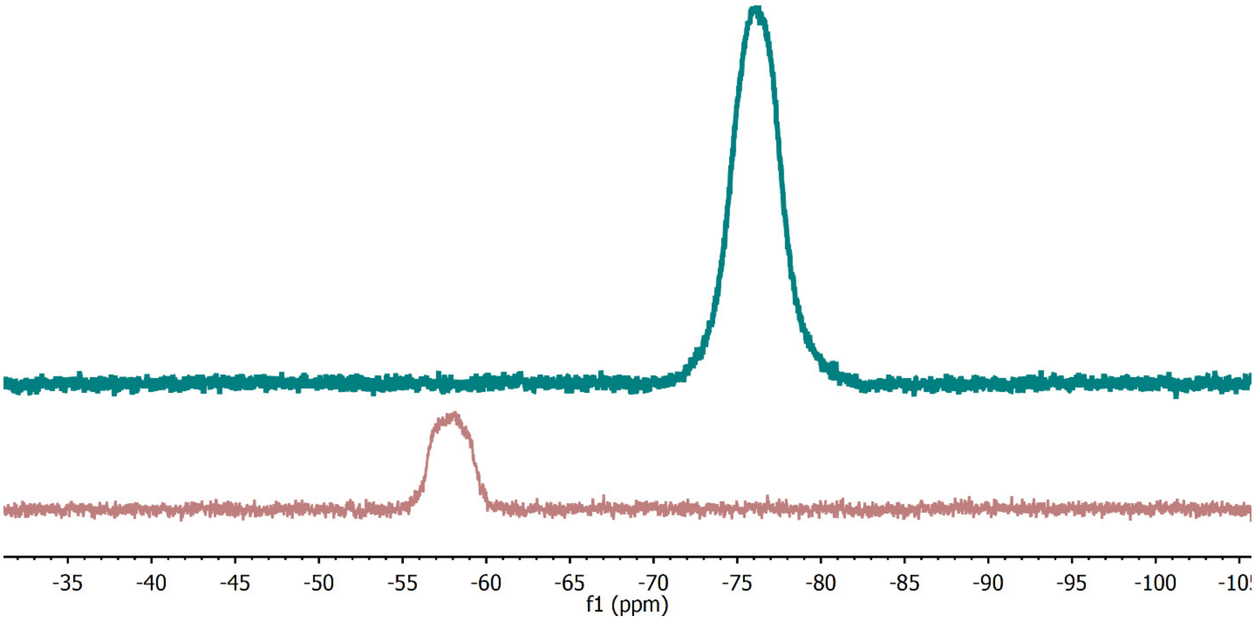

Figure S9. ^{19}F{^{1}H} NMR of **2** in THF (bottom) and in the presence of 10 eq LiOTf (top). The shifted and broadened signal supports that OTf^{-} is associating with Ni at least transiently, and the presence of only one signal in the presence of excess OTf^{-} supports that exchange with free OTf^{-} is occurring rapidly on the NMR timescale. These data are consistent with triflate exchange through either a dissociative or an associative mechanism.

UV-vis Spectra

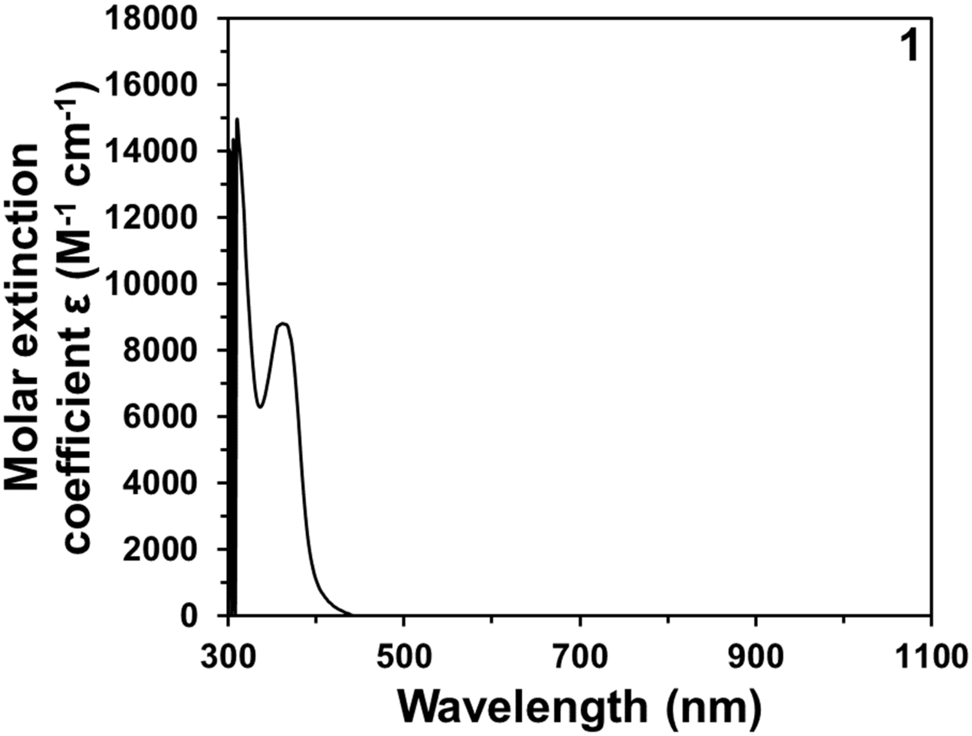

Figure S10. UV-vis of a 0.31 mM solution of **1** in THF.

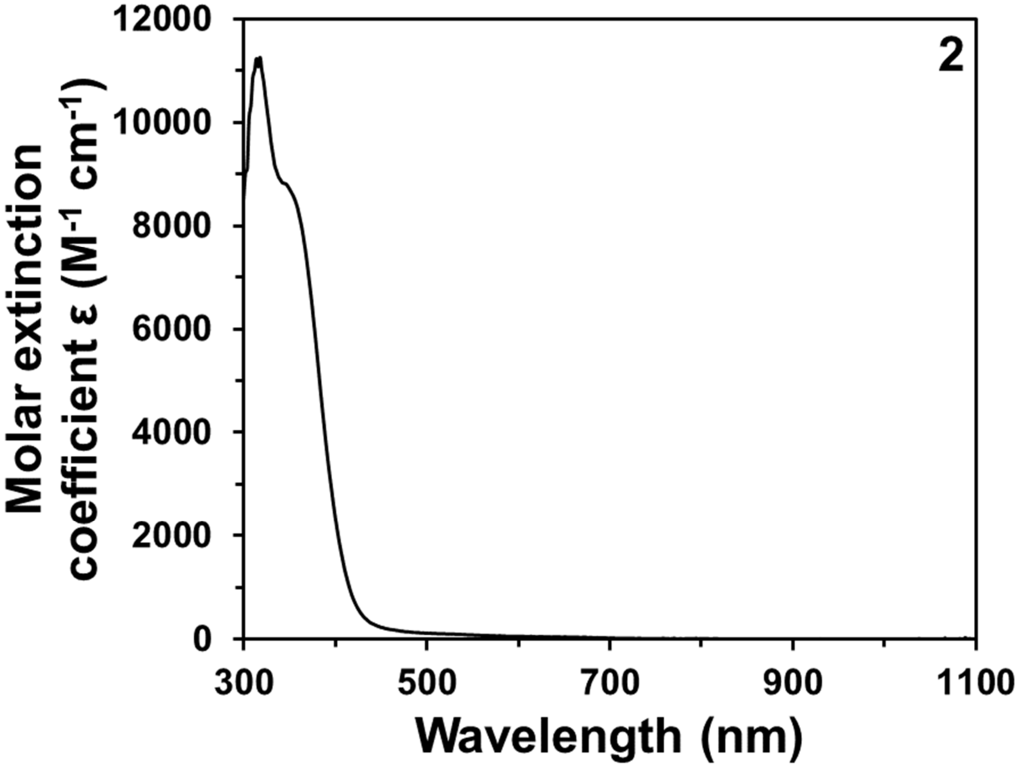

Figure S11. UV-vis of a 0.25 mM solution of **2** in THF.

IR Spectra

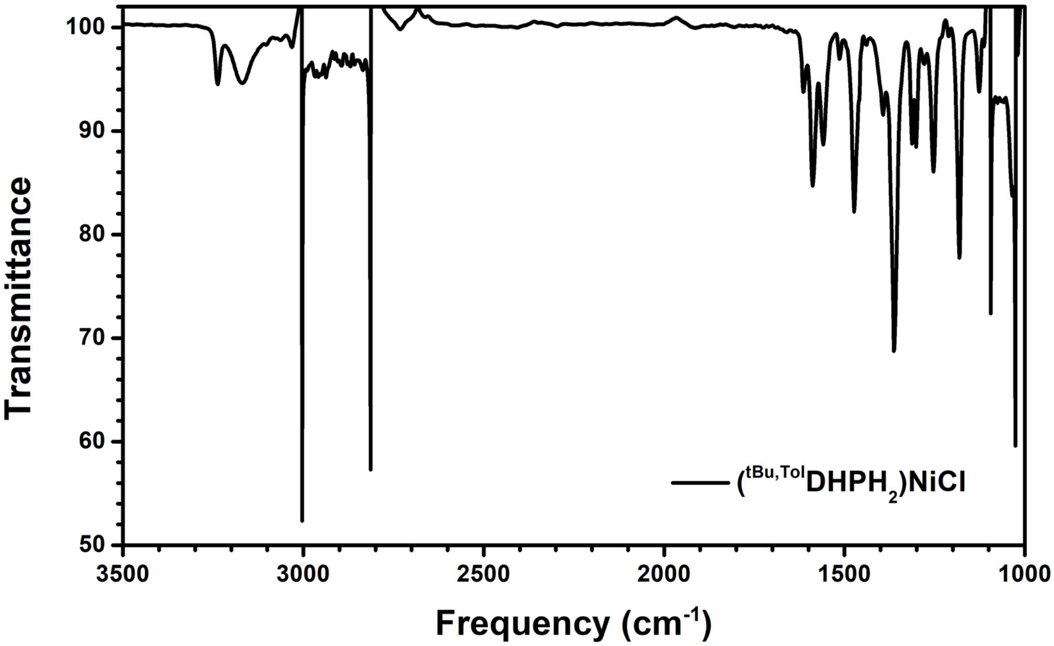

Figure S12. IR (THF solution, CaF$_2$ windows) of **1**. The large features at ~3000 and 1100 cm^{-1} are from an imperfect solvent subtraction.

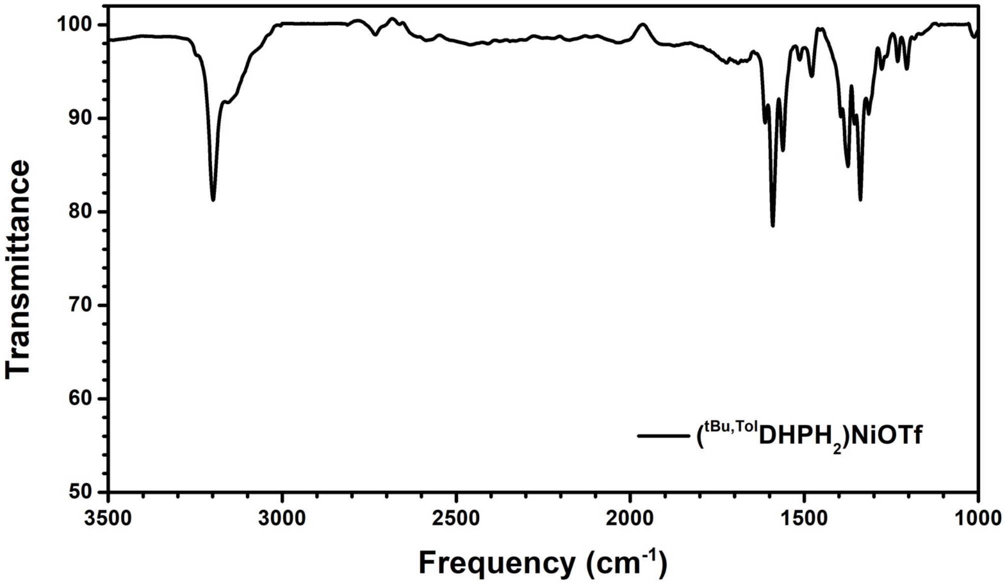

Figure S13. IR (THF solution, CaF$_2$ windows) of **2**.

Kinetics Studies

To report an Eyring analysis, the rate constant k must be calculated.

For a reaction where:

$$\text{Rate} = k[H_2][Ni]$$

under pseudo-first order conditions (i.e. $[H_2] >>> [Ni]$), one can simplify the rate to:

$$\text{Rate} = k_{obs}[Ni]$$

This means that $[H_2]$ is included in k_{obs}, and thus

$$k = k_{obs}/ [H_2]$$

In the experimental setup, 0.5 mL of H_2 gas was added to a UV-vis cuvette with 2 mL of reaction mixture in THF and 2 mL of headspace. This should result in a partial pressure of 0.2 atm H_2 at equilibrium. The reaction was stirred for the duration of the experiment, such that it is reasonable to assume that equilibrium was achieved within minutes of H_2 addition. $[H_2]$ in THF was estimated using mole fraction data at varying pressure and temperatures (E. Brunner, *J. Chem. Eng. Data*, 1985, **30**, 269–273.). The mole fraction at 298.15 K at varying H_2 pressures was plotted and a linear fit was determined (Figure S12). This was repeated for the published data at 323.15 K (Figure S12). The slopes of these lines were then plotted versus temperature and a linear fit was determined, where the slope is in units of mole fraction $H_2{*}MPa^{-1}{*}K^{-1}$ (Figure S12). This trendline was used to calculate the mole fraction H_2 per atm H_2 at the temperatures used in the Eyring analysis. Given that the temperature range used is relatively small, the linear fit used in this calculation should be a reasonable approximation. From there, the partial pressure of H_2 was used to calculate the mole fraction at a given temperature. This was then used to determine the concentration of H_2 in solution, and subsequently the rate constant (see Table S1 and S2 for calculated values).

The rates calculated were then used for the Eyring analysis to give a line of best fit with an R^2 value of 0.99:

$$y = -7024.59934x + 14.84064$$

Error in the y-intercept used to determine $\Delta S^{\ddagger}$ was determined by assuming plus or minus one order of magnitude in the mole fraction of H_2. This resulted in $\Delta S^{\ddagger} = -18\pm5$ cal/mol.

Error in the slope used to determine $\Delta H^{\ddagger}$ was determined by propagation of error in the line of best fit (i.e. error in the slope calculated for the line of best fit). This resulted in $\Delta H^{\ddagger} = 13.9\pm0.4$ kcal/mol

This analysis requires the following assumptions:

1) The $[H_2]$ in the (stirred) solution was at equilibrium within minutes of H_2 addition.
2) The mole fraction of H_2 per atm in THF will correlate in a linear fashion to temperature within a limited temperature range.

3) [Ni] is dilute enough that it will not influence the [H_2].

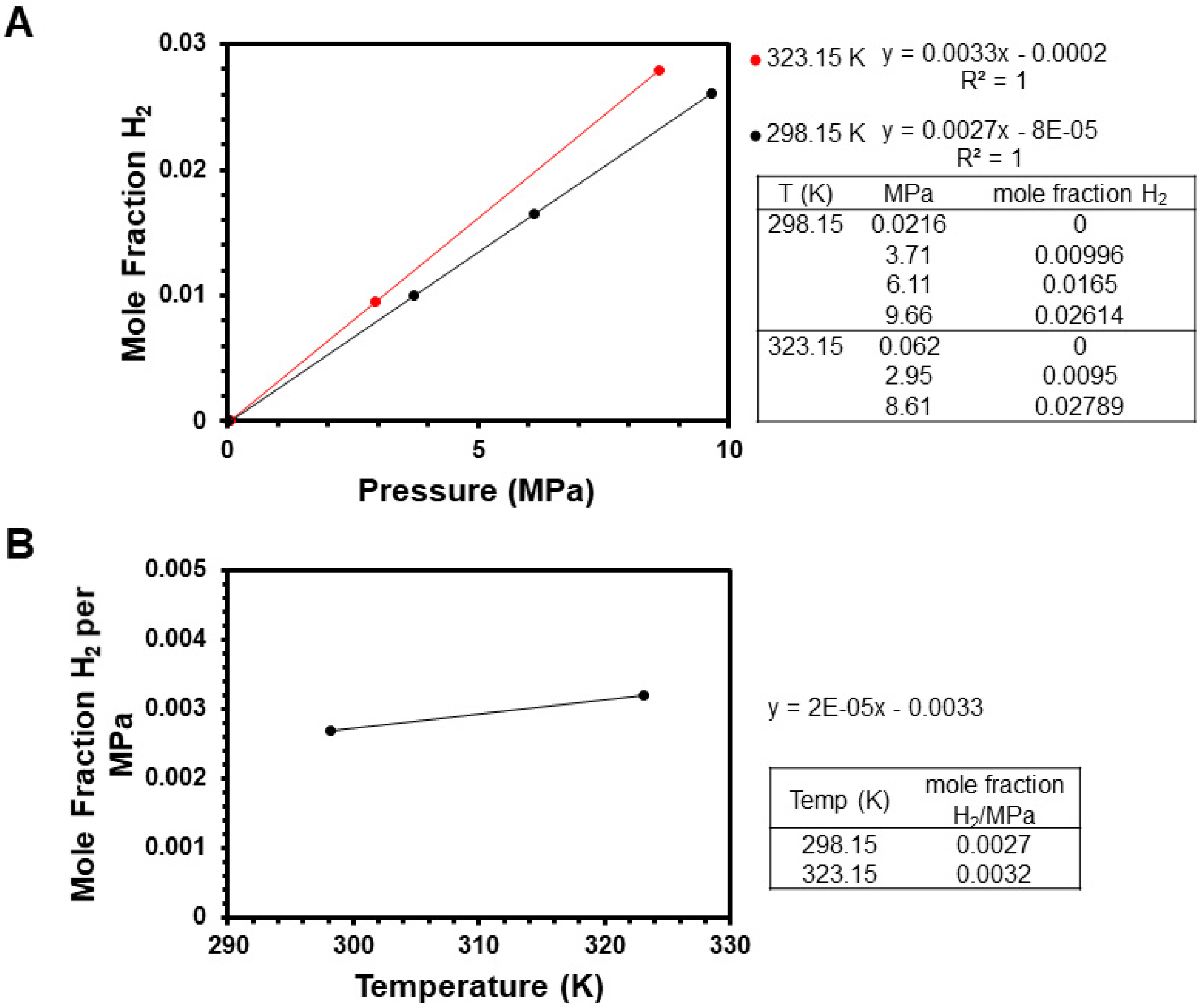

T (K)	MPa	mole fraction H_2
298.15	0.0216	0
	3.71	0.00996
	6.11	0.0165
	9.66	0.02614
323.15	0.062	0
	2.95	0.0095
	8.61	0.02789

Temp (K)	mole fraction H_2/MPa
298.15	0.0027
323.15	0.0032

Figure S14. (A) Determination of the mole fraction of H_2 at variable pressure at a given temperature. (B) Determination of the mole fraction per MPa and temperature.

Table S1. Calculation of [H_2] in UV-vis samples.

T (K)	mole fraction H_2/MPa	mole fraction H_2/atm	mole fraction H_2 (0.2 partial pressure)	moles THF (in 2 mL)	moles H_2	[H_2] (M)
303	0.00276	0.000279657	5.59E-05	0.0246568	1.38E-06	0.00069
313	0.00296	0.000299922	6.00E-05		1.48E-06	0.00074
323	0.00316	0.000320187	6.40E-05		1.58E-06	0.00079
333	0.00336	0.000340452	6.81E-05		1.68E-06	0.00084

Table S2. Rates of reaction of **3** with H_2 at 650 nm.

Sample	[Ni] (mM)	Temp (K)	k_{obs} (s^{-1})	[H2] at 0.2 atm partial pressure	k ($M^{-1}s^{-1}$)	average k ($M^{-1}s^{-1}$)
60-1	0.4	333	0.0004793	0.000839502	0.570885934	0.628939385
60-2	0.2		0.000562		0.669449106	
60-3	0.2		0.0005427		0.646483115	
50-1	0.4	323	0.0002788	0.000789529	0.353152486	0.340871741
50-2	0.4		0.0002885		0.365364836	
50-3	0.4		0.0002401		0.3040979	
40-1	0.4	313	0.0001277	0.000739555	0.172691576	0.167812069
40-2	0.4		0.0001176		0.159042837	
40-3	0.4		0.000127		0.171701793	
30-1	0.2	303	4.57E-05	0.000689583	0.066205981	0.074499149
30-2	0.4		6.33E-05		0.091715757	
30-3	0.4		4.96E-05		0.071893044	
30-4	0.4		4.70E-05		0.068181814	

Table S3. Calculated data for the Eyring Analysis at 650 nm.

1/T (K^{-1})	average ln(k/T)	Standard Deviation
0.003003	−6.274167219	0.083714763
0.003096	−6.887515759	0.097647693
0.003195	−7.593751103	0.045965973
0.0033	−8.413692173	0.148299394

Table S4. Rates of **3** to **2** under pseudo first-order conditions at 50 °C

Conditions	k_{obs} (s^{-1})
Benzene	0.00035061
THF, 50 eq LiOTf	0.000290449

Table S4 shows that no significant change in rate occurs in non-coordinating solvent or in the presence of excess triflate. These observations suggest that there is not a rate-contributing triflate dissociation step during the reaction.

Table S5. Raw data for kinetic studies at 650 nm at 60 °C.

60-1, 0.2 mM		60-2, 0.4 mM		60-3, 0.2 mM	
time (s)	absorbance	time (s)	absorbance	time (s)	Absorbance
0	1.890283195	0	3.570384856	0	1.832635219
1800	0.854176401	300	3.136487697	300	1.620444971
3600	0.35957588	600	2.759195736	600	1.399083991
5400	0.165227704	900	2.352544066	900	1.171749601
7200	0.093990015	1200	2.002209621	1200	0.970275385
9000	0.063683872	1500	1.688591921	1500	0.799313844
10800	0.053140115	1800	1.416001979	1800	0.651953986
12600	0.049813534	2100	1.186452367	2100	0.528372595
14400	0.049195837	2400	0.991261272	2400	0.424442436
16200	0.047926218	2700	0.829063138	2700	0.338263428
18000	0.047479822	3000	0.692275977	3000	0.268178025
19800	0.048096229	3300	0.577724536	3300	0.20931287
21600	0.047971323	3600	0.48255444	3600	0.16208952
23400	0.047984793	3900	0.404004137	3900	0.121984548
25200	0.047938539	4200	0.333918358	4200	0.092899858
27000	0.048805522	4500	0.279035844	4500	0.063892178
28800	0.048686157	4800	0.231211151	4800	0.041540117
30600	0.046955981	5100	0.192333457	5100	0.029283975
32400	0.046029091	5400	0.159673438	5400	0.006733981
34200	0.046629939	5700	0.132064186	5700	-0.005051218
36000	0.047033108	6000	0.113600984	6000	-0.015234615
37800	0.04603749	6300	0.089617688	6300	-0.023890332
39600	0.046488859	6600	0.073063581	6600	-0.030545321
		6900	0.062025061	6900	-0.036479596
		7200	0.049606076	7200	-0.039705178

Table S6. Raw data for kinetic studies at 650 nm at 50 °C.

50-1, 0.4 mM		50-2, 0.4 mM		50-3, 0.4 mM	
time (s)	absorbance	time (s)	absorbance	time (s)	Absorbance
0	4.008520458	0	3.977733347	0	XXX.XXX
600	3.385814201	600	3.522644038	600	3.821428501
1200	2.990883534	1200	2.96763303	1200	3.260752605
1800	2.566842292	1800	2.54012253	1800	2.844134553
2400	2.206073521	2400	2.150226372	2400	2.497876592
3000	1.878159566	3000	1.819146901	3000	2.181618155
3600	1.596820922	3600	1.533352766	3600	1.89146839
4200	1.35760805	4200	1.285371519	4200	1.633021059
4800	1.16778466	4800	1.07884437	4800	1.399530712
5400	1.012741187	5400	0.903982607	5400	1.193846489
6000	0.885591141	6000	0.757269686	6000	1.017217501
6600	0.763098019	6600	0.63464645	6600	0.862676371
7200	0.658425248	7200	0.532661024	7200	0.732801049
7800	0.5857333	7800	0.447448177	7800	0.623136744
8400	0.509079025	8400	0.37874074	8400	0.530511221
9000	0.453117413	9000	0.320568194	9000	0.453227332
9600	0.408541065	9600	0.272603577	9600	0.390945466
10200	0.360368057	10200	0.2345189	10200	0.337873759
10800	0.322829661	10800	0.202502109	10800	0.292830801
11400	0.293687	11400	0.176945582	11400	0.257984091
12000	0.26568	12000	0.156766195	12000	0.228254934
12600	0.242049354	12600	0.141815644	12600	0.203863654
13200	0.223385211	13200	0.126016532	13200	0.185494188
13800	0.209577671	13800	0.11643304	13800	0.169578277
14400	0.195279779	14400	0.108135145	14400	0.15719953

Table S7. Raw data for kinetic studies at 650 nm at 40 °C.

40-1, 0.4 mM		40-2, 0.4 mM		40-3, 0.4 mM	
time (s)	absorbance	time (s)	absorbance	time (s)	Absorbance
0	4.392795508	0	3.933200333	0	3.481915845
600	3.65695004	900	4.163802073	900	2.969607959
1200	3.346371695	1800	3.425020986	1800	2.689605514
1800	3.112726848	2700	3.145668641	2700	2.46146734
2400	2.927998613	3600	2.848209411	3600	2.252023224
3000	2.715295711	4500	2.541259214	4500	2.077044406
3600	2.513855645	5400	2.26882784	5400	1.922379095
4200	2.345193263	6300	2.026873084	6300	1.788993321
4800	2.166494931	7200	1.803169996	7200	1.67167419
5400	2.002556683	8100	1.602821126	8100	1.561031519
6000	1.846734789	9000	1.420456288	9000	1.472844616
6600	1.703140495	9900	1.256309392	9900	1.395500597
7200	1.566636842	10800	1.108332755	10800	1.322488141
7800	1.441505477	11700	0.97759465	11700	1.255843888
8400	1.322050597	12600	0.860115085	12600	1.198266029
9000	1.213868125	13500	0.757161938	13500	1.144215202
9600	1.113677274	14400	0.66688717	14400	1.094239457
10200	1.025673636	15300	0.587287521	15300	1.050259082
10800	0.942061645	16200	0.518159929	16200	1.009190912
11400	0.866776546	17100	0.45734472	17100	0.969797284
12000	0.796556375	18000	0.404665635	18000	0.936218128
12600	0.735007097	18900	0.357890801	18900	0.90395764
13200	0.67488927	19800	0.318243351	19800	0.872167771
13800	0.622193688	20700	0.28415098	20700	0.841748009
14400	0.572568278	21600	0.25340203	21600	0.815197211
15000	0.528170468				
15600	0.487197658				
16200	0.449958078				
16800	0.414333458				
17400	0.384476375				
18000	0.355717056				
18600	0.330194749				
19200	0.306347093				
19800	0.284503808				
20400	0.265042285				
21000	0.245580391				
21600	0.231392008				
22200	0.215755274				

Table S8. Raw data for kinetic studies at 650 nm at 30 °C.

30-1, 0.2 mM		30-2, 0.4 mM		30-3, 0.4 mM		30-4, 0.4 mM	
time (s)	absorbance	time (s)	absorbance	time (s)	Absorbance	time (s)	absorbance
0	2.194978723	0	5.732766758	0	5.210163346	0	XXX.XXX
1800	2.035520154	1800	4.190530172	1800	4.112193101	3600	XXX.XXX
3600	1.878928855	3600	4.559967371	3600	3.84332777	7200	3.657142625
5400	1.722835163	5400	3.885274666	5400	3.357662994	10800	2.999521464
7200	1.583581452	7200	3.341032134	7200	3.112714935	14400	2.550484801
9000	1.455933701	9000	2.986444374	9000	2.873172733	18000	2.185895985
10800	1.339635038	10800	2.73211702	10800	2.628095644	21600	1.872093196
12600	1.235433361	12600	2.518407118	12600	2.389502075	25200	1.601460762
14400	1.138126435	14400	2.294030042	14400	2.186333871	28800	1.339885623
16200	1.029800232	16200	2.087604205	16200	1.98953023	32400	1.1059832
18000	0.955531271	18000	1.895394113	18000	1.814140409	36000	0.902342431
19800	0.881349719	19800	1.72596645	19800	1.651720997	39600	0.735387251
21600	0.808513967	21600	1.570130941	21600	1.504924262	43200	0.569649785
23400	0.745006601	23400	1.412090808	23400	1.369276824	46800	0.455533063
25200	0.685163718	25200	1.273856065	25200	1.245337841	50400	0.363926982
27000	0.633188444	27000	1.148043778	27000	1.132833842	54000	0.284568404
28800	0.585816374	28800	1.041253072	28800	1.030156849	57600	0.234786188
30600	0.539630049	30600	0.944358089	30600	0.935867496	61200	0.200872981
32400	0.496986538	32400	0.856449349	32400	0.851094029	64800	0.169077985
34200	0.456434748	34200	0.758919894	34200	0.771148491	68400	0.152240146
36000	0.420932602	36000	0.690711792	36000	0.699981978	72000	0.137240421
37800	0.380948623	37800	0.619243528	37800	0.632956063	75600	0.130512776
39600	0.345459885	39600	0.563841097	39600	0.573046668	79200	0.123308909
41400	0.312201655	41400	0.512972713	41400	0.516603241	82800	0.118942723
43200	0.28452183	43200	0.469458667	43200	0.465519207		

Table S9. Reaction rates used to calculate KIE at 650 nm.

Sample	Concentration (mM)	rate (s^{-1})	Average rate (s^{-1})	Standard Deviation
50-D2-1	0.4	−0.000320895	–0.000329324	1.06104E−05
50-D2-2	0.2	−0.000325839		
50-D2-3	0.2	−0.000341239		
50-1	0.4	−0.000278824	–0.000269128	2.56022E−05
50-2	0.4	−0.000288466		
50-3	0.4	−0.000240094		

Table S10. Raw data for kinetic studies with D_2 at 650 nm.

50-D2-1		50-D2-2		50-D2-3	
time (s)	abs	time (s)	abs	time (s)	abs
0	3.907567	0	2.289456	0	0.629055
3600	1.456463	1800	1.248725	1800	0.869496
7200	0.494954	3600	0.608157	3600	0.796192
10800	0.131833	5400	0.286295	5400	0.645058
14400	0.012704	7200	0.124566	7200	0.496543
18000	-0.015046	9000	0.040619	9000	0.375564
21600	-0.027081	10800	−0.013676	10800	0.294881
25200	-0.032393	12600	−0.050722	12600	0.22183
28800	-0.035543	14400	−0.074521	14400	0.175633
32400	-0.036263	16200	−0.089433	16200	0.14742
36000	-0.037009	18000	−0.098289	18000	0.128091
39600	-0.037608	19800	−0.103808	19800	0.111909
43200	-0.038501	21600	−0.107162	21600	0.102503
46800	-0.037347	23400	−0.109999	23400	0.09368
		25200	−0.11113	25200	0.088158
		27000	−0.111644	27000	0.089144
		28800	−0.113592	28800	0.088502
		30600	−0.112553	30600	0.085427
		32400	−0.113556	32400	0.083101
		34200	−0.113836	34200	0.083009
		36000	−0.113611	36000	0.084996
		37800	−0.114223	37800	0.086547
		39600	−0.113619	39600	0.085229
		41400	−0.114231		
		43200	−0.113527		

DFT Calculations

Geometry Optimizations

Structures were optimized in ORCA using the B3P functional and def2-TZVPP basis set on Ni, def2-TZVP basis set on all other atoms.[5,6,7] Frequency calculations were performed to confirm the structures are the lowest point on the potential energy surface. For calculation of the thermodynamics of H_2 splitting, the cationic species were calculated in the absence of triflate counterions.

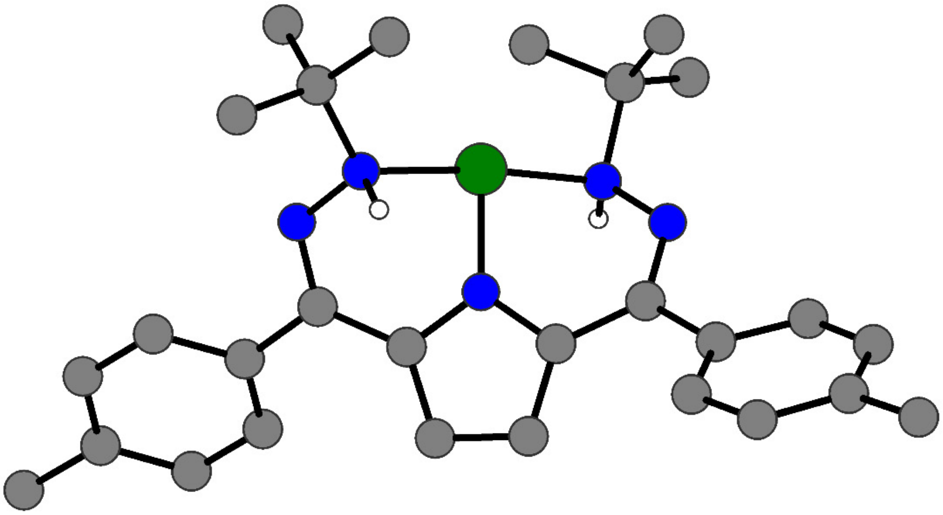

Figure S15. Calculated structure of **2**$^+$.

Table S11. Coordinates of calculated structure of **2**$^+$.

N	−1.4404	−0.1138	−0.4046
C	−2.5281	−0.934	−0.3909
C	−2.0656	−2.2576	−0.313
C	−0.6735	−2.2067	−0.2622
C	−0.3029	−0.8541	−0.3397
H	0.0072	−3.0439	−0.2149
H	−2.685	−3.1401	−0.2592
Ni	−1.5164	1.6797	−0.6611
C	1.0007	−0.2097	−0.3863
N	1.2137	0.956	−0.9239
N	0.1268	1.5484	−1.5974
C	0.3614	2.9926	−1.9612
C	1.1235	3.684	−0.8403
H	0.6501	3.5168	0.1318
H	1.1473	4.7592	−1.0321
H	2.1456	3.3147	−0.7759

C	−1.0723	3.5299	−2.0457
H	−1.6147	3.4667	−1.0577
H	−1.6661	3.0546	−2.8309
H	−1.0947	4.6094	−2.2176
C	1.0868	3.1104	−3.2907
H	2.0718	2.6435	−3.2281
H	1.2264	4.1616	−3.554
H	0.5247	2.6332	−4.0997
N	−3.0996	1.6068	0.4762
N	−4.1372	0.861	−0.1285
C	−3.8657	−0.3649	−0.4603
C	−5.0164	−1.1358	−0.9623
C	2.1665	−0.7985	0.2927
C	−6.2958	−0.7993	−0.5129
C	−7.4135	−1.4266	−1.0288
C	−7.3014	−2.4134	−2.0082
C	−6.0211	−2.7579	−2.4464
C	−4.8938	−2.1354	−1.9322
H	−6.4038	−0.0335	0.2453
H	−8.3964	−1.1462	−0.6636
H	−5.9052	−3.5187	−3.2125
H	−3.9157	−2.4043	−2.3157
C	−8.5209	−3.0714	−2.5771
H	−9.4302	−2.7257	−2.0737
H	−8.4659	−4.1634	−2.4741
H	−8.6187	−2.8416	−3.6482
C	3.4576	−0.4334	−0.1013
C	4.556	−0.8064	0.6501
C	4.4092	−1.5479	1.824
C	3.1239	−1.9524	2.1861
C	2.0171	−1.5893	1.4367
H	3.5872	0.1689	−0.9923
H	5.5483	−0.5009	0.333
H	1.028	−1.8732	1.7773
H	2.9843	−2.5336	3.0922
C	−3.6618	2.8358	1.1623
C	−2.4878	3.547	1.826
H	−1.9708	2.8986	2.5411
H	−2.8522	4.4165	2.3758
H	−1.7572	3.9085	1.0953
C	−4.3524	3.7284	0.1451
H	−3.6509	4.1508	−0.5797
H	−4.8273	4.5647	0.6621
H	−5.1192	3.174	−0.3971
C	−4.6489	2.3649	2.2283

H	−4.1631	1.695	2.9467
H	−5.4901	1.8386	1.7763
H	−5.0347	3.2233	2.7824
C	5.5924	−1.8886	2.6763
H	6.4541	−1.2562	2.4411
H	5.8959	−2.9336	2.5248
H	5.3556	−1.7629	3.7393
H	−2.696	1.0396	1.2313
H	−0.0708	1.0173	−2.4519

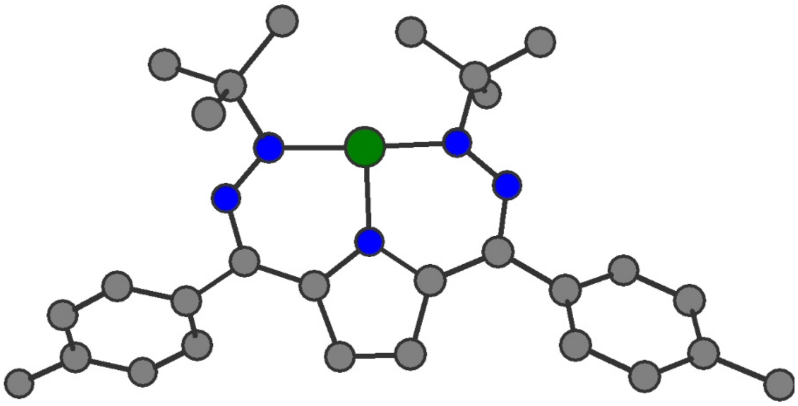

Figure S16. Calculated structure of **3**$^+$.

Table S12. Coordinates of calculated structure of **3**$^+$.

N	−1.80341	0.1806	−0.14201
C	−2.84915	−0.66817	−0.21687
C	−2.35948	−2.02091	−0.23045
C	−0.99881	−1.94566	−0.17401
C	−0.66037	−0.54644	−0.12135
Ni	−1.92218	2.08054	−0.06365
C	0.60256	0.08883	−0.12574
N	0.78205	1.36594	−0.55234
N	−0.10186	2.26254	−0.58412
C	0.35722	3.46843	−1.36182
C	1.61931	4.04055	−0.72062
H	1.45176	4.28974	0.33027
H	1.90598	4.95458	−1.24542
H	2.44558	3.33135	−0.78466
C	−0.77645	4.47968	−1.30951
H	−0.86138	4.93455	−0.31968
H	−1.73283	4.00727	−1.57259
H	−0.60977	5.28024	−2.03307
C	0.62714	3.02999	−2.80209

H	1.39716	2.25626	−2.83309
H	0.97621	3.88439	−3.38602
H	−0.27758	2.63532	−3.2734
N	−3.7423	1.99763	0.47226
N	−4.51598	1.01778	0.30776
C	−4.17907	−0.17505	−0.24177
C	−5.31433	−0.89136	−0.79348
C	1.85814	−0.57103	0.20156
C	−6.61917	−0.54204	−0.39934
C	−7.71779	−1.08682	−1.0282
C	−7.57404	−1.99695	−2.07853
C	−6.27676	−2.37442	−2.44781
C	−5.1683	−1.83752	−1.82388
H	−6.75113	0.16228	0.41131
H	−8.7128	−0.79637	−0.707
H	−6.13929	−3.07717	−3.26357
H	−4.17846	−2.09952	−2.18022
C	−8.76735	−2.53735	−2.79711
H	−9.68726	−2.05975	−2.45978
H	−8.86549	−3.61643	−2.63608
H	−8.67522	−2.37687	−3.87614
C	3.05438	−0.10676	−0.374
C	4.26875	−0.64721	−0.01197
C	4.35456	−1.65983	0.94507
C	3.1634	−2.13179	1.51364
C	1.93929	−1.60465	1.15077
H	3.00931	0.67372	−1.12123
H	5.17699	−0.2764	−0.4752
H	1.03983	−1.95251	1.64631
H	3.20487	−2.90931	2.27026
C	−4.3528	3.0611	1.34636
C	−3.3447	4.19643	1.43091
H	−2.37418	3.84181	1.79957
H	−3.69327	4.96107	2.12772
H	−3.20783	4.67349	0.45722
C	−5.65166	3.55042	0.70694
H	−5.47793	3.93222	−0.30256
H	−6.06785	4.36113	1.30869
H	−6.38622	2.74621	0.65356
C	−4.62332	2.45992	2.72665
H	−3.70548	2.07958	3.18336
H	−5.34089	1.6401	2.65763
H	−5.0409	3.22819	3.38095
C	5.68536	−2.20342	1.35574
H	6.4955	−1.7242	0.80618
H	5.74399	−3.28225	1.17887
H	5.85789	−2.03841	2.42471
H	−2.96227	−2.91549	−0.26949
H	−0.30136	−2.76934	−0.17545

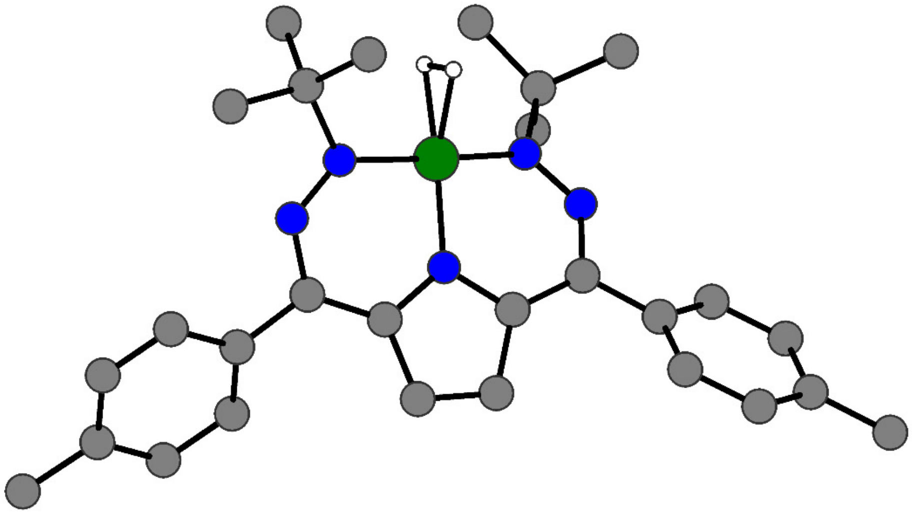

Figure S17. Calculated structure of an H_2 adduct of **3**$^+$.

Table S13. Coordinates of structure of an H_2 adduct of **3**$^+$.

N	−1.8048	0.3158	−0.0838
C	−2.8639	−0.5113	−0.2966
C	−2.3862	−1.8695	−0.3389
C	−1.0431	−1.8281	−0.164
C	−0.6712	−0.4424	−0.0191
Ni	−1.8689	2.1248	0.1694
C	0.6085	0.1096	0.0222
N	0.8124	1.4004	−0.3053
N	−0.0704	2.2973	−0.3824
C	0.5273	3.5415	−1.0578
C	1.7615	3.9852	−0.2762
H	1.5017	4.2638	0.7491
H	2.1984	4.8614	−0.7605
H	2.5114	3.1955	−0.244
C	−0.4567	4.6987	−1.1462
H	−0.6429	5.1748	−0.1806
H	−1.4048	4.4108	−1.6124
H	−0.0159	5.4672	−1.7852
C	0.8985	3.1096	−2.4803
H	1.626	2.297	−2.4643
H	1.3386	3.9556	−3.0125
H	0.016	2.7749	−3.0329
N	−3.7251	2.0626	0.5161
N	−4.5146	1.1637	0.1174
C	−4.175	−0.0422	−0.3802

C	−5.2921	−0.8053	−0.9444
C	1.8347	−0.6633	0.2505
C	−6.605	−0.561	−0.5156
C	−7.673	−1.2143	−1.0975
C	−7.4854	−2.1429	−2.127
C	−6.1795	−2.3893	−2.5475
C	−5.1014	−1.7322	−1.975
H	−6.7772	0.1502	0.2827
H	−8.6778	−1.0021	−0.7446
H	−6.0055	−3.0903	−3.3574
H	−4.1078	−1.9061	−2.3733
C	−8.6507	−2.8285	−2.7713
H	−9.2981	−2.1053	−3.2778
H	−9.2654	−3.3459	−2.0289
H	−8.3248	−3.5609	−3.5112
C	3.0238	−0.2935	−0.3891
C	4.1949	−0.9912	−0.1661
C	4.2343	−2.0854	0.7002
C	3.0502	−2.4444	1.3484
C	1.8719	−1.7483	1.1342
H	3.0206	0.5475	−1.0712
H	5.1019	−0.6805	−0.6751
H	0.9834	−2.0261	1.6914
H	3.0557	−3.2732	2.0496
C	−4.4661	3.206	1.2127
C	−4.4338	4.4524	0.3251
H	−3.4355	4.8651	0.1621
H	−5.0227	5.2398	0.8021
H	−4.8806	4.2395	−0.6487
C	−5.9296	2.8309	1.4392
H	−6.4603	2.6807	0.5
H	−6.4073	3.6502	1.9806
H	−6.0266	1.9253	2.0409
C	−3.8187	3.444	2.5783
H	−2.8026	3.8433	2.5329
H	−3.798	2.5216	3.1627
H	−4.4148	4.1757	3.1278
C	5.5054	−2.8476	0.9183
H	6.3754	−2.2546	0.6304
H	5.5163	−3.761	0.3149
H	5.6206	−3.1504	1.9617
H	−3.0087	−2.7418	−0.4621
H	−0.353	−2.6572	−0.1643
H	−1.9702	3.7144	0.2792
H	−1.7254	3.4777	0.9746

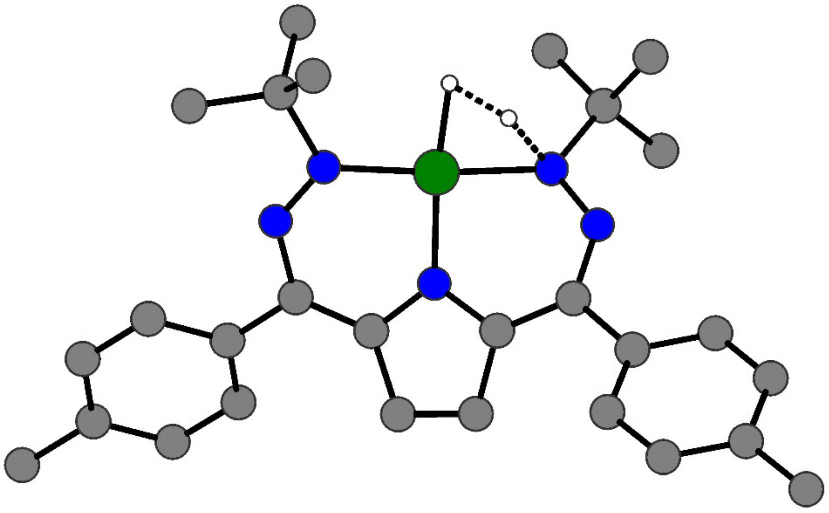

Figure S18. Calculated structure of transition state 1.

Table S14. Coordinates of calculated transition state 1.

N	−1.8051	0.3255	−0.2155
C	−2.9133	−0.4102	−0.3617
C	−2.5516	−1.8077	−0.3125
C	−1.2012	−1.8663	−0.1687
C	−0.7265	−0.5047	−0.113
Ni	−1.8071	2.1638	−0.0887
C	0.561	0.0165	−0.0952
N	0.8309	1.3172	−0.4568
N	0	2.2471	−0.5698
C	0.6231	3.5206	−1.1194
C	0.5779	4.5787	−0.0169
H	−0.4407	4.8081	0.298
H	1.03	5.4988	−0.3933
H	1.1469	4.2535	0.8573
C	−0.1939	3.9378	−2.341
H	−1.2343	4.1569	−2.0951
H	−0.1681	3.163	−3.1114
H	0.245	4.845	−2.7622
C	2.0717	3.2952	−1.5352
H	2.7042	3.027	−0.6885
H	2.447	4.2274	−1.9628
H	2.1601	2.5168	−2.2959
N	−3.6294	2.2193	0.4839

N	−4.52	1.3618	−0.0036
C	−4.2209	0.1726	−0.4763
C	−5.3474	−0.5906	−1.0434
C	1.7656	−0.7561	0.1749
C	−6.6606	−0.3239	−0.6367
C	−7.7262	−0.9859	−1.2139
C	−7.5328	−1.9395	−2.2203
C	−6.2263	−2.1989	−2.6253
C	−5.1496	−1.5373	−2.051
H	−6.8359	0.4153	0.1354
H	−8.7335	−0.7607	−0.8768
H	−6.0472	−2.9199	−3.4163
H	−4.1511	−1.7351	−2.4262
C	−8.6946	−2.6437	−2.852
H	−9.3479	−1.9346	−3.3703
H	−9.3044	−3.1534	−2.1002
H	−8.3638	−3.3868	−3.5791
C	2.9848	−0.3784	−0.4107
C	4.1369	−1.0978	−0.1691
C	4.1328	−2.2162	0.6677
C	2.9223	−2.5783	1.27
C	1.7616	−1.8672	1.0339
H	3.0124	0.4785	−1.0705
H	5.064	−0.7869	−0.6397
H	0.854	−2.1433	1.5586
H	2.8987	−3.4221	1.9524
C	−4.2897	3.192	1.4605
C	−5.2445	4.1026	0.6953
H	−4.7048	4.7263	−0.0258
H	−5.7576	4.7724	1.3901
H	−5.993	3.5161	0.16
C	−5.042	2.3636	2.4975
H	−5.8217	1.7589	2.0358
H	−5.512	3.0431	3.2129
H	−4.3626	1.7058	3.0466
C	−3.2161	4.0039	2.17
H	−2.7212	4.7222	1.5141
H	−2.4619	3.3565	2.6253
H	−3.697	4.5757	2.9671
C	5.3835	−2.9999	0.9095
H	6.269	−2.4364	0.6114
H	5.3712	−3.9285	0.3292
H	5.4851	−3.2817	1.9604
H	−3.2425	−2.6338	−0.3782
H	−0.5872	−2.7525	−0.1376

H	−3.06	3.1153	−0.2687
H	−2.0446	3.659	−0.2176

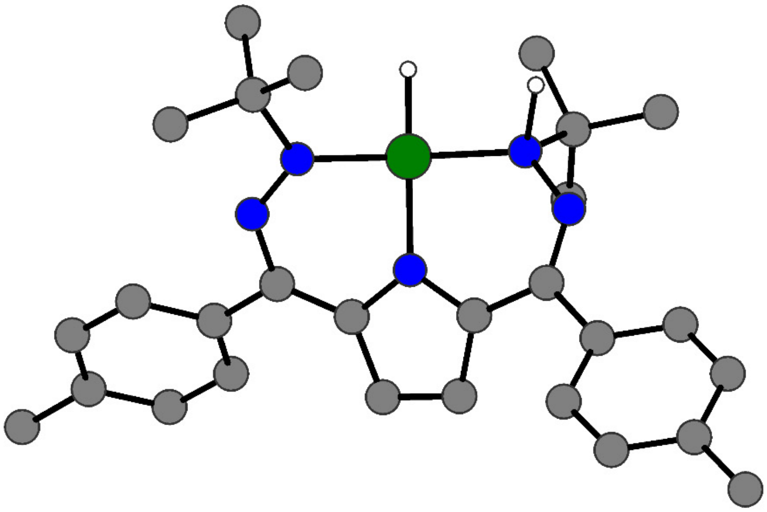

Figure S19. Calculated structure of a Ni-hydride intermediate.

Table S15. Coordinates of a calculated Ni-hydride intermediate.

N	−1.8922	0.5242	−0.3582
C	−3.0242	−0.1569	−0.3457
C	−2.7644	−1.5481	−0.0935
C	−1.4143	−1.6732	0.0509
C	−0.8623	−0.356	−0.1054
Ni	−1.7267	2.393	−0.1541
C	0.4457	0.1011	−0.0962
N	0.7687	1.3082	−0.6941
N	0.0169	2.2922	−0.7847
C	0.6074	3.4072	−1.6224
C	1.0863	4.483	−0.6461
H	0.2635	4.8697	−0.0443
H	1.5163	5.3052	−1.2227
H	1.8599	4.0886	0.0176
C	−0.5021	3.9377	−2.5252
H	−1.3394	4.3249	−1.9415
H	−0.8679	3.1636	−3.2049
H	−0.1018	4.7567	−3.127
C	1.7812	2.9082	−2.4532
H	2.6275	2.6206	−1.829

H	2.1063	3.7202	−3.1063
H	1.5025	2.0586	−3.0809
N	−3.614	2.5748	0.2836
N	−4.5742	1.7434	−0.3756
C	−4.3068	0.5082	−0.61
C	−5.3842	−0.28	−1.2418
C	1.6102	−0.6369	0.3497
C	−6.7243	0.0107	−0.9674
C	−7.7375	−0.6754	−1.6082
C	−7.4546	−1.6633	−2.5582
C	−6.118	−1.9444	−2.8321
C	−5.0943	−1.2708	−2.1824
H	−6.9597	0.7847	−0.247
H	−8.7702	−0.4381	−1.3717
H	−5.8734	−2.6974	−3.5741
H	−4.0652	−1.4983	−2.442
C	−8.5559	−2.3932	−3.2635
H	−9.2004	−1.6974	−3.8095
H	−9.192	−2.9303	−2.5531
H	−8.1606	−3.1178	−3.9772
C	2.8687	−0.3504	−0.2101
C	3.9943	−1.0324	0.1993
C	3.9242	−2.0246	1.1807
C	2.6748	−2.2934	1.7551
C	1.5393	−1.619	1.3537
H	2.9407	0.3938	−0.9916
H	4.9511	−0.7984	−0.2558
H	0.5979	−1.8166	1.8526
H	2.601	−3.0358	2.5435
C	−4.0465	2.8312	1.7395
C	−5.5249	3.2241	1.7627
H	−5.7218	4.0657	1.0947
H	−5.7957	3.5334	2.7746
H	−6.1744	2.4002	1.4693
C	−3.8081	1.5665	2.544
H	−4.3984	0.7279	2.1681
H	−4.1143	1.7402	3.5788
H	−2.7523	1.2832	2.545
C	−3.2181	3.9894	2.2806
H	−3.3214	4.8806	1.6569
H	−2.1588	3.7402	2.3505
H	−3.5836	4.2408	3.2797
C	5.1445	−2.7868	1.5857
H	6.0544	−2.2253	1.3673
H	5.2004	−3.7297	1.0309

H	5.1317	−3.0403	2.648
H	−3.5073	−2.3304	−0.0487
H	−0.8564	−2.583	0.2083
H	−3.8913	3.754	−0.2869
H	−1.572	3.81	0.1607

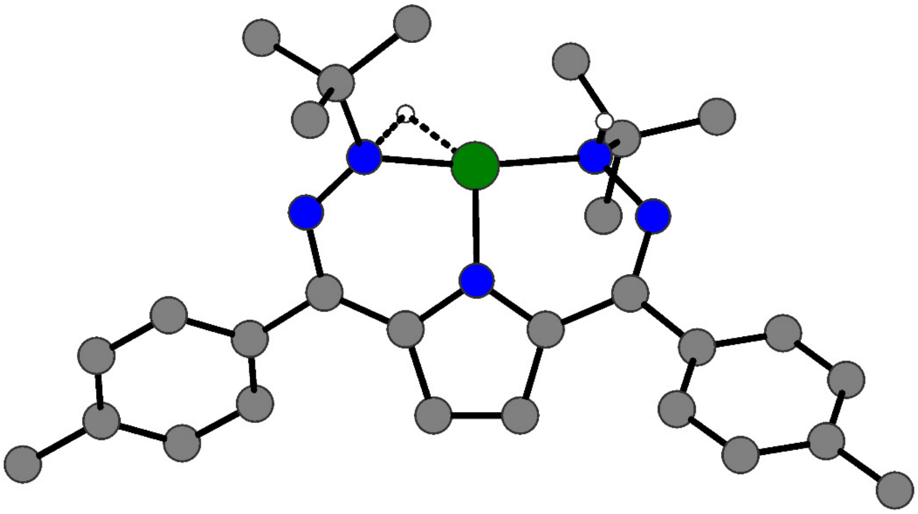

Figure S20. Calculated structure of transition state 2.

Table S16. Coordinates of the calculated structure of transition state 2.

N	−1.8621	0.5013	−0.5155
C	−2.9832	−0.2099	−0.4703
C	−2.6566	−1.5748	−0.2197
C	−1.2909	−1.6453	−0.0905
C	−0.7888	−0.3193	−0.2298
Ni	−1.7429	2.3026	−0.298
C	0.5157	0.192	−0.0948
N	0.8723	1.4373	−0.4989
N	0.0037	2.3528	−0.7106
C	0.5084	3.4881	−1.5728
C	1.7082	4.1387	−0.8942
H	1.4386	4.5272	0.0918
H	2.0562	4.9752	−1.5038
H	2.5247	3.4261	−0.7792
C	−0.6356	4.4807	−1.729
H	−0.8885	4.9693	−0.783
H	−1.5296	4.0025	−2.1478
H	−0.3425	5.2625	−2.4319
C	0.8927	2.8946	−2.9289
H	1.6871	2.1553	−2.8199
H	1.2546	3.6942	−3.5783

H	0.0348	2.4186	−3.4115
N	−3.6209	2.5475	0.1952
N	−4.5785	1.6537	−0.4105
C	−4.2817	0.4275	−0.6893
C	−5.3698	−0.365	−1.2944
C	1.6463	−0.594	0.3961
C	−6.7058	−0.076	−0.9969
C	−7.7292	−0.754	−1.6294
C	−7.4617	−1.7348	−2.5915
C	−6.1298	−2.0203	−2.8822
C	−5.0954	−1.353	−2.2425
H	−6.9297	0.6924	−0.2666
H	−8.7587	−0.5159	−1.3773
H	−5.8971	−2.7704	−3.6308
H	−4.0712	−1.5796	−2.5151
C	−8.5748	−2.4503	−3.293
H	−9.2164	−1.7447	−3.8302
H	−9.2111	−2.9858	−2.5816
H	−8.1916	−3.1736	−4.0144
C	2.9367	−0.2887	−0.0599
C	4.0346	−0.9824	0.4064
C	3.9011	−1.9967	1.3557
C	2.6172	−2.2848	1.8291
C	1.5088	−1.6051	1.3594
H	3.064	0.4911	−0.7992
H	5.0201	−0.7339	0.0257
H	0.5358	−1.8219	1.7843
H	2.4884	−3.0475	2.5911
C	−4.0391	2.8489	1.6456
C	−5.5085	3.2668	1.6639
H	−5.6968	4.092	0.9651
H	−5.7708	3.6139	2.6655
H	−6.1706	2.4431	1.4002
C	−3.8131	1.6246	2.5171
H	−4.413	0.7785	2.1779
H	−4.1159	1.8529	3.5402
H	−2.7618	1.3275	2.5308
C	−3.1772	4.0171	2.1016
H	−3.3223	4.894	1.4605
H	−2.115	3.7596	2.1119
H	−3.4651	4.3055	3.1142
C	5.0945	−2.7422	1.8605
H	6.0103	−2.4058	1.3748
H	4.9882	−3.8167	1.6798
H	5.2121	−2.6028	2.9403
H	−3.3603	−2.3931	−0.1774
H	−0.7036	−2.5337	0.0795
H	−3.7466	3.1043	−0.1124
H	−0.6166	3.0647	0.496

Table S17. Free energies of calculated complexes and Mulliken Charges of H as H_2 is split.

	Free Energy		Mulliken Charge	
Complex*	Hartrees	kcal/mol	H68	H69
H_2	−1.18105314	−740.52031878	-	-
LNi + H_2	0	0	-	-
LNi(H_2)	0.01736033	10.9370079	0.01	0.08
TS1	0.04502982	28.3687866	0.10	−0.10
(LH)NiH	0.01280404	8.0665452	0.26	−0.06
TS2	0.04111216	25.9006608	0.25	0.02
(LH_2)Ni	−0.01029469	−6.4856547	0.25	0.26

*all complexes are cationic with the triflate removed for ease of calculation

Kinetic Isotope Effects

To assess the consistency of the proposed mechanism with the experimentally observed inverse KIE we estimated the semiclassical transition state using our DFT optimized structures and vibrational calculations. Enthalpies and entropies at 323 K were calculated using the formula of an ideal gas, assuming all rotations as rigid rotors and all vibrations as harmonic oscillators.[8] Performing these calculations for both isotopomers gave ΔH, TΔS, and ΔG values for the losses of enthalpy, entropy, and free energy upon deuteration for each species. The ΔH values are all positive whereas the TΔS values are all negative, reflecting how deuterated isotopomers contain less zero point energy and a larger number of thermally available configurations. These tendencies reinforce to give positive ΔG for all species. The difference between the ΔG of two species gives a ΔΔG value, which represents the change in relative free energy between the two species upon deuteration. When these two species are the reactant and a transition state (or product), the semiclassical isotope effect is $\exp(-\Delta\Delta G/kT)$. A positive value of ΔΔG indicates an inverse isotope effect and a negative value indicates a normal isotope effect. The elementary step of H_2 splitting (i.e. progression of $LNiH_2$ to TS1) is estimated to have a normal KIE; however, an inverse isotope effect is estimated for the binding of H_2. This analysis suggests that the entire reaction has a calculated isotope effect near unity, as determined experimentally (although a small normal effect is estimated rather whereas a small inverse effect is observed). Furthermore, these calculations suggest that the origin of the inverse isotope dependence is from H_2 association, as might be expected for an EIE.

Table S18. Calculated free energy differences between H_2 and D_2 isotopomers at 323 K.

Species	ΔH = H(H_2) – H(D_2)	TΔS = TS(H_2) – TS(D_2)	ΔG = ΔH – TΔS
Free H_2	1.83 kcal/mol	-1.10 kcal/mol	2.93 kcal/mol
$LNiH_2$	2.90 kcal/mol	-0.57 kcal/mol	3.47 kcal/mol
TS1	2.48 kcal/mol	-0.33 kcal/mol	2.81 kcal/mol

Table S19. Calculated isotope effect (IE) at 323 K.

Starting Species	Final Species	ΔΔG = ΔG(Final) – ΔG(Start)	IE = exp(–ΔΔG / RT)
Free H_2	$LNiH_2$	+0.54 kcal/mol	0.4
Free H_2	TS1	-0.12 kcal/mol	1.2
$LNiH_2$	TS1	-0.66 kcal/mol	2.8
	Experimental	+0.3 kcal/mol	0.8

X–ray Crystallography

Table S20. Crystal structure and refinement data for **1** and **2**.

Identification code	**1**	**2**
Empirical formula	$C_{33}H_{48}ClN_5Ni$	$C_{29}H_{36}F_3N_5NiO_3S$
Formula weight	608.92	650.40
Temperature/K	100(2)	100(2)
Crystal system	triclinic	Monoclinic
Space group	P–1	$P2_1/c$
a/Å	10.3991(5)	9.57352(3)
b/Å	11.3467(5)	19.2736(6)
c/Å	15.9639(8)	16.4544(4)
α/°	90.377(2)	90
β/°	106.279(2)	94.3950(10)
γ/°	115.5700(10)	90
Volume/Å^3	1613.26(13)	3078.30(15)
Z	2	4
ρ_{calc}g/cm^3	1.254	1.403
μ/mm^{-1}	0.714	0.181
F(000)	652.0	1360.0
Crystal size/mm^3	0.59 × 0.47 × 0.34	0.2 × 0.1 × 0.1
Radiation	MoKα (λ = 0.71073)	synchrotron (λ = 0.41328)
2Θ range for data collection/°	4.498 to 52.874	1.896 to 34.38
Index ranges	$-13 \leq h \leq 13$, $-14 \leq k \leq 14$, $-19 \leq l \leq 19$	$-13 \leq h \leq 13$, $-27 \leq k \leq 27$, $-23 \leq l \leq 22$
Reflections collected	34504	119850
Independent reflections	6628 [R_{int} = 0.0325, R_{sigma} = 0.0278]	9365 [R_{int} = 0.0523, R_{sigma} = 0.0209]
Data/restraints/parameters	6628/0/371	9365/0/387
Goodness–of–fit on F^2	1.049	1.061
Final R indexes [I>=2σ (I)]	R_1 = 0.0445, wR_2 = 0.1135	R_1 = 0.0290, wR_2 = 0.0832
Final R indexes [all data]	R_1 = 0.0555, wR_2 = 0.1197	R_1 = 0.0322, wR_2 = 0.0852
Largest diff. peak/hole / e Å^{-3}	1.50/–0.72	0.46/–0.61

Mass Spectrometry

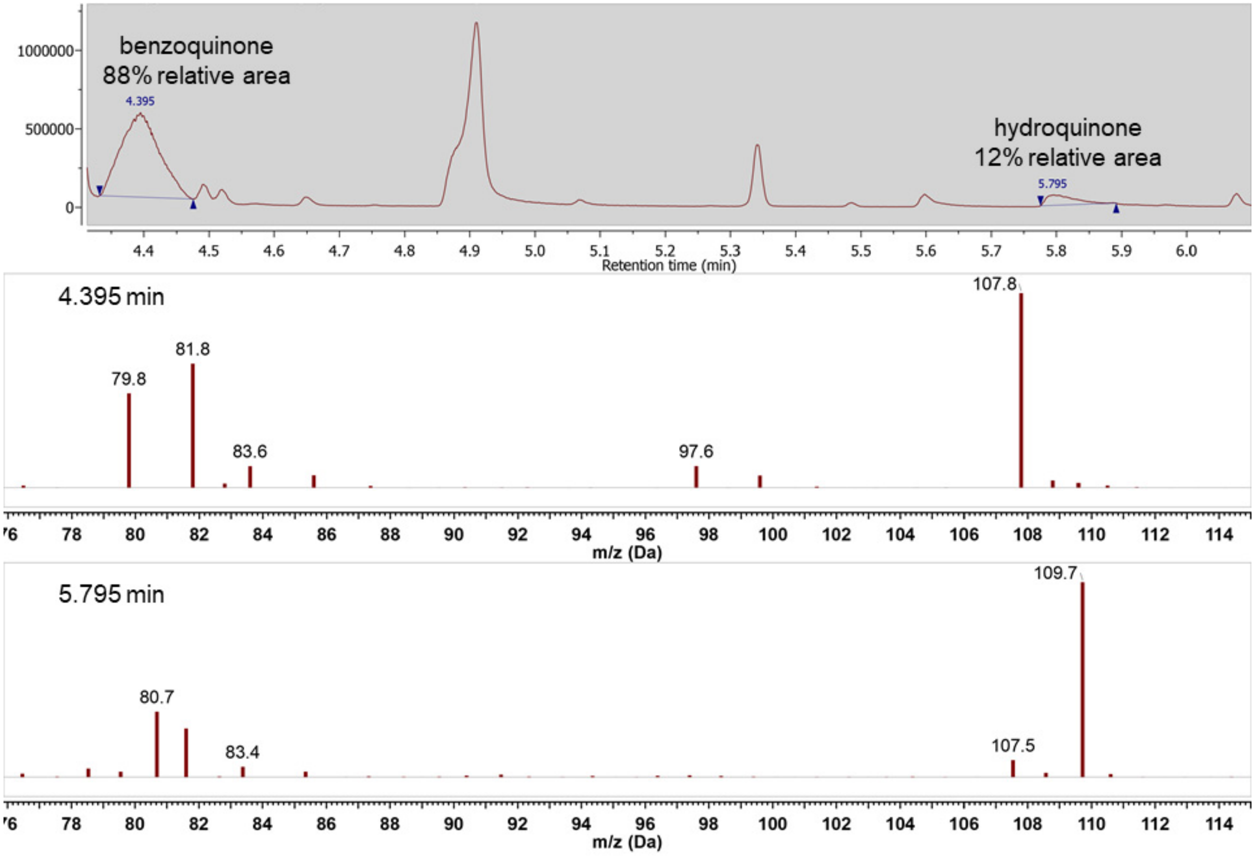

Figure S21. GC-MS of the catalytic hydrogenation of benzoquinone (20 eq) by **3** (1 eq.) in d_8-toluene under 1 atm H_2 at room temperature over 7 days. The relative integration of peaks corresponding to the protonated benzoquinone and hydroquinone are approximately 9:1, indicating a TON of ~2.

References

1 A. J. McNeece, K. A. Jesse, J. Xie, A. S. Filatov, J. S. Anderson. *J. Am. Chem. Soc.* **2020**, *142*, 10824-10832
2. G. M. Sheldrick. *Acta Cryst***. 2015**, *A71*, 3- 9
3. O. V. Dolomanov, L. J. Bourhis, R. J. Gildea, A. K. Howard, H. Puschmann, *J. Appl. Cryst*. **2009**. *42*, 339
4. (a) G. M. Sheldrick. *Acta Cryst*. **2008***, A64*, 112-122; (b) G. M. Sheldrick, *Acta Cryst*. **2015,** *C71*, 3-8
5. F. Neese, Wiley interdisciplinary Reviews - Computational Molecular Science, **2012**, *2* (1), 73–78.
6. F. Weigend and R. Ahlrichs, *Phys. Chem. Chem. Phys.*, 2005, **7**, 3297–3305.
7. F. Weigend, *Phys. Chem. Chem. Phys.*, 2006, **8**, 1057–1065.
8. T. L. Hill, *An Introduction to Statistical Thermodynamics.*, Dover Publications, Newburyport, 2012.